BULLETIN OF THE POLISH ACADEMY OF SCIENCES
TECHNICAL SCIENCES, Vol. 68, No. 1, 2020
DOI: 10.24425/bpasts.2020.131837

Low voltage modular circuit breakers: FEM employment for modelling of arc chambers

Ł. KOLIMAS, S. ŁAPCZYŃSKI, M. SZULBORSKI*, and M. ŚWIETLIK

Institute of Electrical Power Engineering, Warsaw University of Technology, 75 Koszykowa St., 00-662 Warsaw, Poland

Abstract. FEM (finite element method) is an essential and powerful numerical method that can explicitly optimize the design process of electrical devices. In this paper, the employment of FEM tools such as SolidWorks, COMSOL and ANSYS is proposed in order to aid electrical apparatuses engineering and modeling – those are arc chambers of modular circuit breakers. Procured models of arc chambers have been undergoing simulations concerning heating, electric potential distribution, electric charge velocity and traverse paths. The data acquired has been juxta-positioned against experimental data procured in the Short-Circuit Laboratory, Warsaw University of Technology. The reflection of the theoretical approach was clearly noted in the experimental results. Mutual areas of the modeled element expressed the same physical properties and robustness errors when tested under specific conditions – faithfully reflecting those which were experimented with. Moreover, the physical phenomena essential for electrical engineering could be determined already at the model stage. This procedure proved highly valuable during designing/engineering work in terms of material economy.

Key words: miniature circuit breaker (MCB), finite element method (FEM), computational fluid dynamics (CFD), arc chambers.

1. Introduction

Rapidly growing demand for electrical installations composed of high quality electrical components dictates new trends in designing low voltage circuit breakers. The main aim of designing and engineering electrical devices is to create solutions that can vastly improve their electrical and mechanical parameters as well as size and endurance for short-circuit conditions. Modern electrical apparatuses are built in accordance with current standards (e.g. European Standards; IEC 60947). These requirements concern low-voltage circuit breakers (LVCB; MCB). Despite the small sizes of the above-mentioned devices, these are adapted to effectively switch off the overload and short-circuit currents and protect the other elements of the electrical systems such as cables and wires. During the process of extinguishing the electric arc in the circuit breaker, complex physical phenomena occur such as heat released in the arc channel and the formation of electrodynamic forces causing stress affecting the contacts of the circuit breaker. This also affects the structural elements that the device is made of (copper, steel, ferromagnetic elements, bimetals, aluminum, polymers etc.). Those occurrences can cause damage to the breaker after exceeding the critical values of electrical durability or temperature. The key element of the circuit breakers' construction is the electric arc chamber. During switching off of the short-circuit current, the arc chamber is exposed to thermal and dynamic influences which can lead to permanent damage of this element or even the whole circuit breaker. Arc chambers vary in shape, size and the number of ferromagnetic plates from which they are constructed. The greater the number of ferromagnetic plates in the chamber, the greater its ability to extinguish the arc. The value of the minimum voltage upholding the electric arc is reduced between the plates, which in combination with the spatial charge created near the cathode (plates) of each ferromagnetic plate is directly causing its faster extinction. The number of plates in the arc chamber for alternating current is described by the following equation:

$$n \geq \frac{U}{\sqrt{3 \cdot \left(\frac{\delta^2 \cdot U_a^2}{1.5^2 \cdot \tau^2} + \frac{\pi^2 \cdot u_t}{4} \right)}}, \tag{1}$$

U is the voltage peak value between open contacts, U_a is the initial durability near the cathode, u_t is the voltage between a pair of consecutive plates, δ is the factor of irregularity between the plates – approx. 0.5, τ is the factor of amplitude (for power breakers – approx.: 1.7; for the motor breaker – approx.: 1.5).

In order to verify the construction guidelines and the necessity of the solutions chosen, many tests and simulations are carried out that allow for detection of defects and optimization of the arc chamber effectivity at the project stage. Those measures are essential for reducing material take-off and they help improve the arc chamber properties. The usage of FEM (finite element method) simulations is very effective for running multiple analysis concerning electrical, mechanical and material durability aspects. The huge advantage of this method lies in the ability to check complicated scenarios employing various boundary conditions. A good example is a simulation concerning gas pressure distribution on the FSI arc chamber surface by Lijun

*e-mail: mm.szulborski@gmail.com

Manuscript submitted 2019-07-13, revised 2019-11-20, initially accepted for publication 2019-11-26, published in February 2020

Wang and his team, which is shown in Fig. 1 below. In the cited case, the simulation was used for maintaining additional information subjected to measurements of the arc chamber housing deformations [1–6].

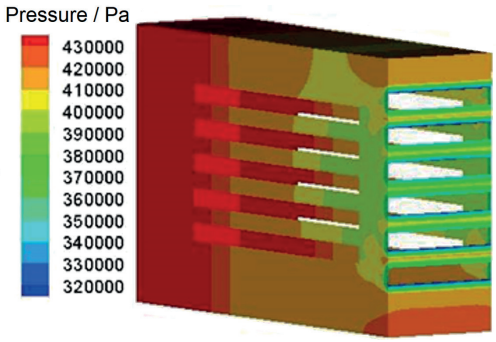

Fig. 1. Pressure distribution on the FSI arc chamber surface [2]

FEM is an essential and powerful numerical method that can explicitly optimize the designing process of electrical devices and proper employment of the finite element method itself. It is the key to arriving at the recipe for easy, fast and precise optimization of arc chamber parameters. This paper focuses on the juxtaposition of experimental data and simulations data in order to show FEM advantages and disadvantages concerning arc chambers modelling parameters – such as the number of plates and critical conditions (temperature, velocity of electrical charge, electrical charge flux in the chamber, electrical potential distribution and overall short-circuit conditions in regard to the materials used). For charge transversal analysis this work employs the usage of various FEM tools like: SolidWorks, Comsol, ANSYS and even computational fluid dynamics (CFD) [7–11].

2. FEM design guidelines

Prompt technological progress allowed for the use of modern software to support the process of designing and engineering electrical apparatuses. Currently constructed electrical appliances are designed and tested with the use of software such as CAD and CAE (Computer Aided Design, Computer Aided Engineering). Mathematical analysis is employed to predict the distribution of electrical fields, temperatures, stresses and other physical quantities. In order to perform such analyzes and simulations, each element is described by specific physical properties, such as: Young's modulus, Poisson's coefficient, thermal expansion ratio, thermal and electrical conductivity. These are the necessary physical properties needed to perform correct calculations during simulations that reflect the actual phenomena occurring in a constructed device. The results of these calculations allow for estimating whether the elements of a designed device, made of specified materials, meet the global standards [12–17].

2.1. AutoCAD (model procurement). AutoCAD software allows for creation of precise 2D technical drawings and 3D three-dimensional models. This functionality is essentially used for drawing elements of the arc chamber. The elements of the structure are matched, which helps generate a simplistic model that is easy to export to other programs, e.g. those that are FEM based. Parts created in the AutoCAD graphical environment are shown in Fig. 2.

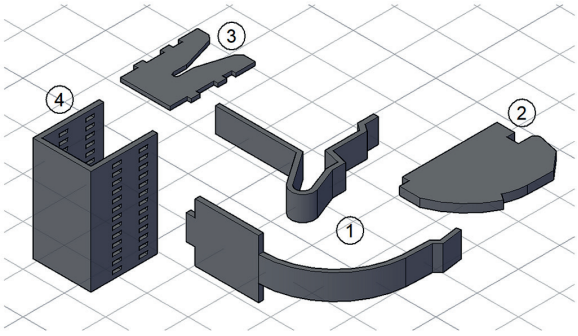

Fig. 2. Elements of the arc chamber created in AutoCAD: 1) tread electrodes; 2) rear sheath; 3) arc chamber plate; 4) arc chamber casing

2.2. COMSOL Multiphysics and SolidWorks (FEM analysis and model procurement). The COMSOL Multiphysics software is a tool with the ability to run and analyze the concurrent simulations of many physical phenomena. The software's key functionality is based on solving partial differential equations using the finite element method (FEM) and molecular dynamics. It is commonly used for electrical analysis concerning potential and electrical field distribution in medium and high voltage devices and systems [18–21].

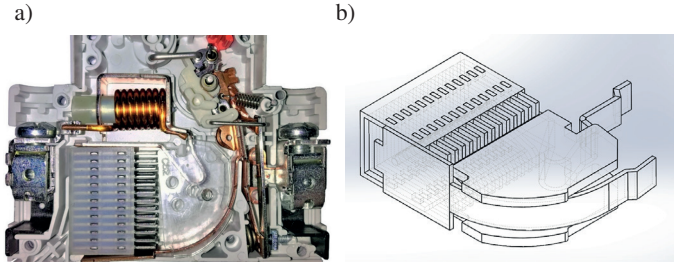

Fig. 3. Visual comparison of a real scale arc chamber (a) and its model drawn in SolidWorks (b)

2.3. ANSYS (advanced FEM analysis). ANSYS is an advanced FEM analytical tool built of various modules that merge into a major multiphysics engine. The use of several conjugate fields makes it possible to visualize the current flow and its effects – not only thermal but also electrodynamic ones. This feature is referred to as "coupling" and it is used regularly for complex analysis of various connected and resulting phenomena [22–24].

The numerical fluid mechanics of the computational fluid dynamics module (CFD; ANSYS module) is a method of simulating the behavior of systems, processes and devices related to the flow of gases and fluids, heat and mass exchange, chemical reactions and other similar physical phenomena. The CFD module allows for obtaining the necessary information about

fluid flow (velocity field distribution, pressure field), heat movement (temperature field) and other accompanying phenomena (including chemical reactions). Electrical analysis can employ CFD in order to simulate potential distribution, electrical charge velocity and its traverse routes inside the chosen element of the analyzed device (arc chamber) [25, 26].

3. FEM simulation results

Mandatory assumptions for all procured simulations were:

- Apparatus modeled: miniature circuit breaker B16/1,
- Number of plates in MCB arc chamber: a) 13 plates; b) 9 plates,
- Voltage parameters: rated voltage: $U_n = 230$ V; voltage,
- Frequency: $f = 50$ Hz; alternating current,
- Breaking capacity: $I_{cu} = 6$ kA; RMS value,
- Simulations were executed in an air surrounding,
- Dimensions of 13 plates in the arc chamber: $14 \times 19.7 \times 26$ mm,
- Dimensions of 9 plates in the arc chamber: $14 \times 19.7 \times 18$ mm,
- Dimensions of single plate: $14 \times 19.7 \times 0.8$ mm.

3.1. Heat distribution in the arc chamber. The simulations performed concerned two variants of the arc chamber, which are shown in Fig. 4 below. Main goal of the simulations was to determine if the distribution of heat in the tested arc chamber models is balanced over the entire element. That would provide data about the path of the electric arc inside the arc chamber during short circuit and its extinguishment. Case a) represents a model of the arc chamber that consists of 13 plates. The even temperature distribution implied that the electric arc was proportionally divided through the metal plates in the arc chamber. Energy dissipation along the metal plates is consistent with the assumptions. Moreover, on the basis of the regular temperature distribution, the proper dynamics of the electric arc propagation on the contact is assumed. The arc was stretched by the moving contacts of tread electrodes (actuator mechanism). It was forced into the arc chamber by tread electrodes and divided thereafter. De-ionization of the intermetallic gap is assumed. In addition, a much lower temperature of rear sheaths provides data about the proper extinguishment of the electric arc. Case b) represents a model of the arc chamber that consists of 9 plates. The temperature distribution is evidently not as balanced as in the case of the 13-plate model of the arc chamber [27, 29–36].

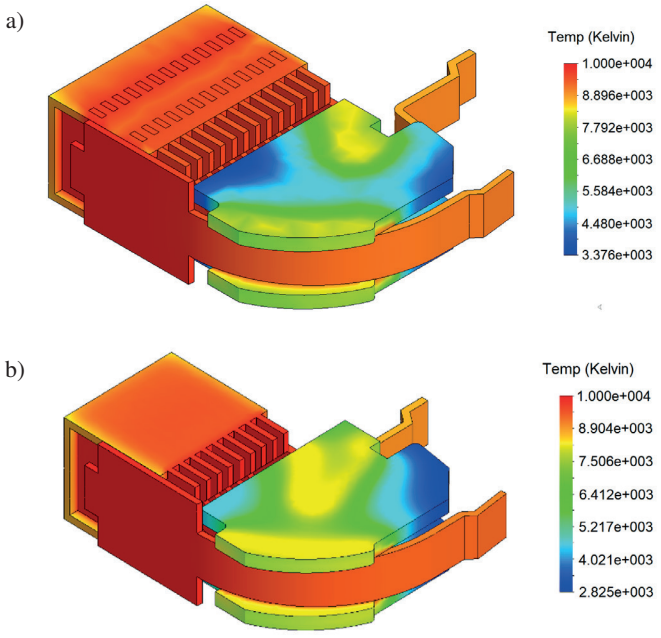

Fig. 4. Simulations of heat distribution (K) for two variants of MCB B16/1 arc chambers: a) arc chamber with 13 plates; b) arc chamber with 9 plates. Simulations were carried out in SolidWorks

Observation concerns mostly the edge of the plates and the tread electrode, where heat values are highest. Other regions of the arc chamber have lower temperatures, which indicate non-exhaustive functioning of the MCB-modeled element. Therefore, the following scenario was possible: the electric arc was not divided completely alongside the length of the modeled element. This may lead to re-ignition of the electric arc at the tread electrode and between the plates. Moreover it would result in welding contact with the arc chamber case, causing vast damage of the apparatus from overheating. The temperature distribution on the rear sheaths indicates that the electric arc was not pushed inside the arc chamber. It could be extinguished on the rear sheath and re-ignited, which applies to the above part, which in turn assumes that the arc was not divided and that the process caused vast damage to the apparatus.

3.2. Electric field and electric potential distribution in the arc chamber. The simulations performed concerned two variants of arc chambers, which are shown in Fig. 5 below. The goal of the simulations was to examine if the electric field distribution is homogenous for both variants and if the electric potential value does not exceed the critical value of 18 V per space located between the single pair of plates installed in the arc chamber, in accordance with experimental data [28].

Both cases present that the distribution of the electric field is not homogenous. The difference in the maximum critical value of the electric field is at least one order of magnitude with advantage on the part of the arc chamber with 13 plates. Moreover, in the 13 plates variant critical values occur on the tread electrodes far from the arc chamber casing, which results from the solution used in electrical connection engineering. It is also unlikely to expect welding of the electrodes. The simulation of the arc chamber with 9 plates shows a higher possibility of welding the electrodes. The critical values are localized much closer to the arc chamber case. It may be assumed that the problem is connected with the lack of control of the electric arc path on the tread electrodes, which is caused by smaller dimensions of the arc chamber. Therefore the distance between the first plate and the electrodes is different for both cases.

Electric potential distribution was valid for both cases and was not different for the 9 and 13 plate variants, as it should be for voltage value of 230 V. Figure 6 presents the electric potential distribution for the variant with 9 plates.

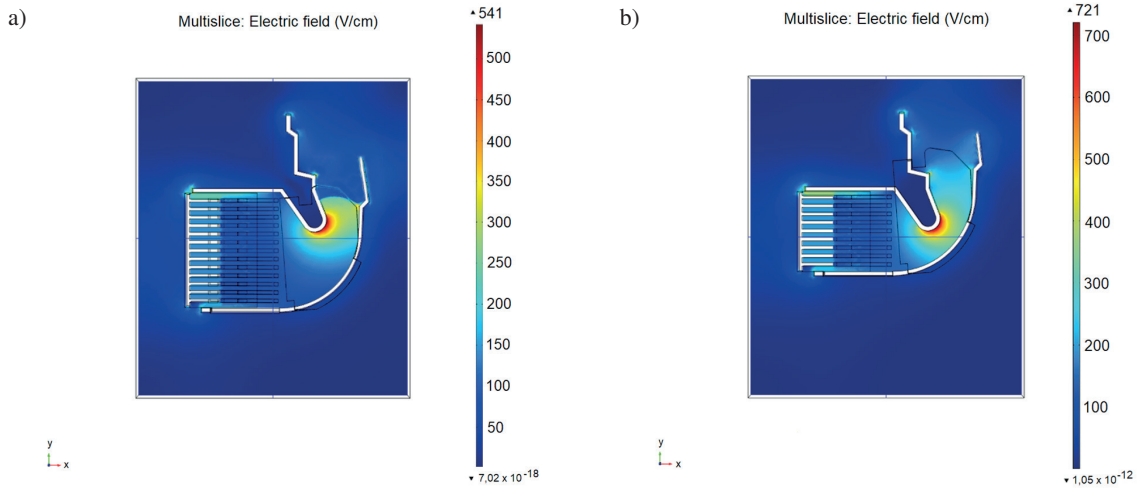

Fig. 5. Simulations of electric field distribution (V/cm) for two variants of MCB B16/1 arc chambers: a) arc chamber with 13 plates; b) arc chamber with 9 plates. Simulations were carried out in Comsol

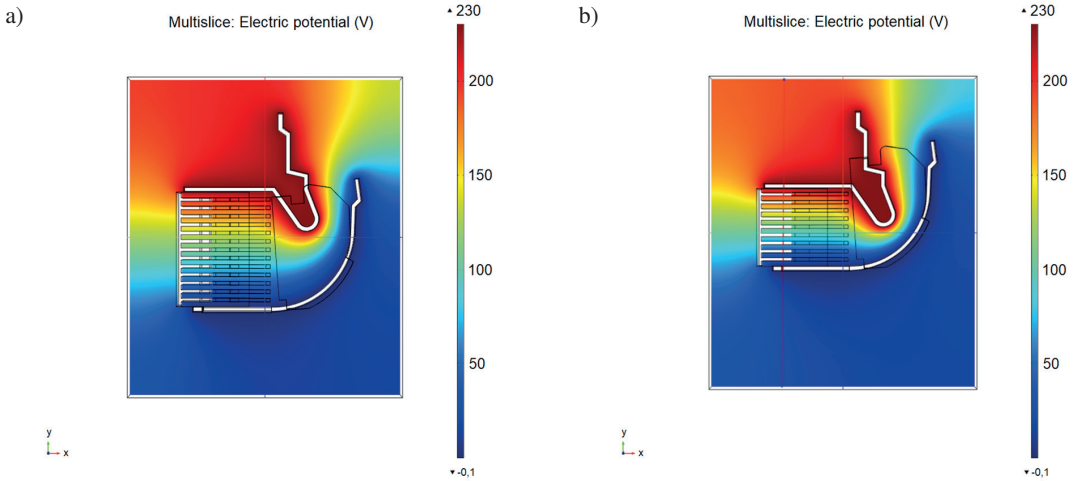

Fig. 6. Simulations of electric potential distribution (V) for two variants of MCB B16/1 arc chambers: a) arc chamber with 13 plates; b) arc chamber with 9 plates. Simulations were carried out in Comsol

Figure 7 shows a comparison of electric values potential between the pairs of plates for the arc chamber variant with 13 plates and 9 plates. The designation line shows the range for which potential was drafted on graphs. It is evident that the potential values for 9 plates are vastly exceeded (values around 26–29 V). Values for the arc chamber with 13 plates are valid

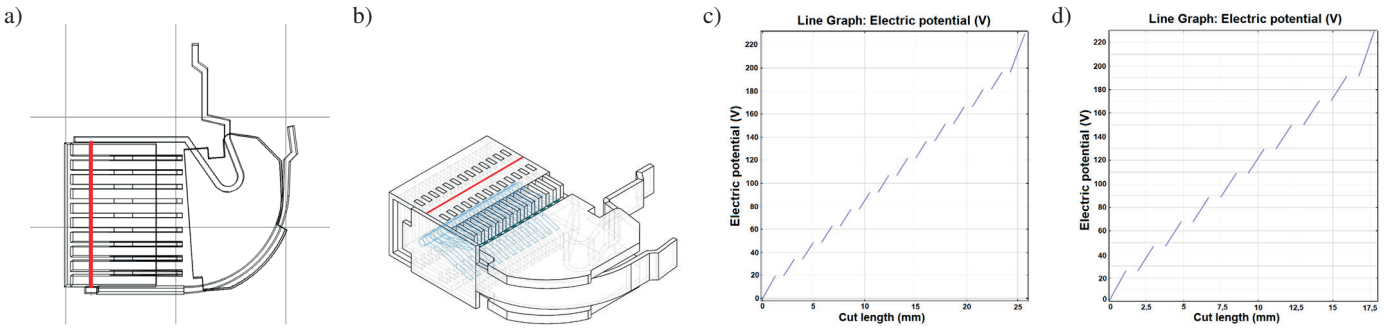

Fig. 7. Graphs presenting values of electric potential (V) dependent on cut length (mm) between the pairs of plates in the arc chambers: a) electric potential designation line (9 plates); b) electric potential designation line (13 plates); c) graph for the arc chamber with 13 plates; d) graph for the arc chamber with 9 plates

(values around 16–18 V). Therefore the applied reduction in the number of plates lacks any physical sense as it may, and probably will, cause errors.

3.3. Velocity and traverse paths of electric charge. The ANSYS analysis was based on the reverse engineered elements drafted in the SolidWorks software. The area representing air present in the gap between the electrodes was generated as a grid of points in which calculations were carried out. For calculation purposes, the source and destination target were defined as surfaces of electrodes facing each other. The initial flow velocity was set as $1.07 \cdot 10^7$ m/s, which is the magnitude of velocity for the elementary charge accelerated at the voltage rate of 230 V. The outcome was the distribution of routes and partial velocities of charges inside the arc chamber in the form of a visualization superimposed on the model. Figure 8 presents particle velocity field distribution and Fig. 9 presents particle flow lines (traverse paths) of the electric charge.

Figure 8 and Fig. 9 indicate highest velocity at areas where the arc is mostly expected. Partial charges colliding with the plates move at a lower velocity before they strike the surface of the other electrode. The combination of traverse paths with the velocity of the electric charge is determinant for the probability of the arc presence in the specific area of the arc chamber.

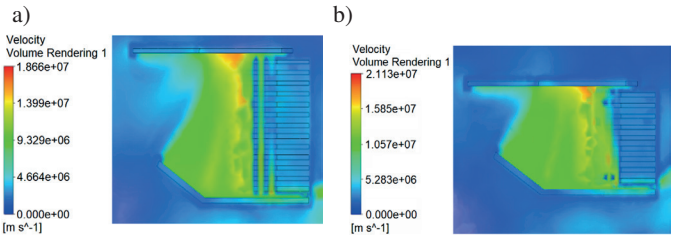

Fig. 8. Particle velocity field distribution for electric charge inside the arc chamber (m/s) for two variants of MCB B16/1 arc chambers: a) arc chamber with 13 plates; b) arc chamber with 9 plates. Simulations were carried out in ANSYS CFD module

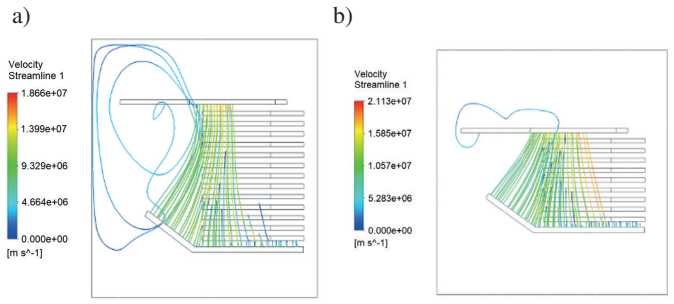

Fig. 9. Traverse paths of electric charge inside the arc chamber for two variants of MCB B16/1 arc chambers: a) arc chamber with 13 plates; b) arc chamber with 9 plates. Simulations were carried out in ANSYS CFD module

The CFD calculation module is originally used to simulate the flow of fluids, therefore obtaining results from it provides interpretation of the electromagnetic phenomena.

The traverse paths of the electric charge in the cross-section of the arc chamber are continuous for the circuit breaker with 13 plates (Fig. 9a). As a result, despite the slightly lower velocity of the particles (in comparison with the chamber with 9 plates), their distribution is regular.

The higher gas pressure in the arc chamber with 9 plates results in higher particle velocity. Bearing in mind the triggering system (electromagnetic coil), this variation of the chamber achieves greater dynamics in relation to the larger, 13-plate arc chamber. The key to effective use of the inter-cathode effect takes the form of even distribution of particles and regular velocity. The studied case shows that it is not fulfilled. This is clearly visible at the arc chamber outset. Numerous discolorations are visible, representing the heterogeneity of electric charge velocity.

4. Laboratory test results

Laboratory tests concerning the two types of the arc chambers were conducted at the Short-Circuit Laboratory forming part of the Electrical Faculty, Warsaw University of Technology. The tests were carried out in accordance with the IEC 60898-1 standard – Electrical accessories – Circuit-breakers for overcurrent protection for household and similar installations – Part 1: Circuit-breakers for a.c. operation. The above-mentioned standard applies to the air circuit breakers for rated voltage not exceeding 440 V, rated current not exceeding 125 A and rated short-circuit breaking capacity not exceeding 25 kA.

In accordance with the standard, two types of overcurrent circuit breakers were tested. The first contained 13 plates in the arc chamber and the second contained 9 plates in the arc chamber, as it was depicted in previous chapter, which concerned FEM simulations. The short-circuit system used during the tests was also shown in Fig. 10.

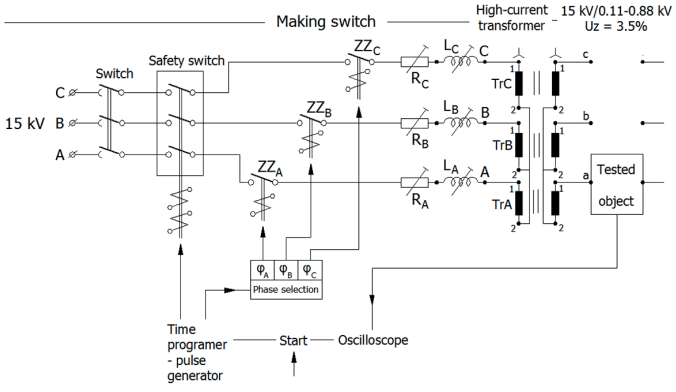

Fig. 10. Short-circuit system used for laboratory tests. Short-Circuit Laboratory, Electrical Faculty, Warsaw University of Technology

4.1. Short-circuit tests. The overcurrent circuit breakers have been tested in accordance with IEC 60898-1. The tests were carried out using single phase from the laboratory short-circuit system. The effective value of the reference current was 6 kA (ref-

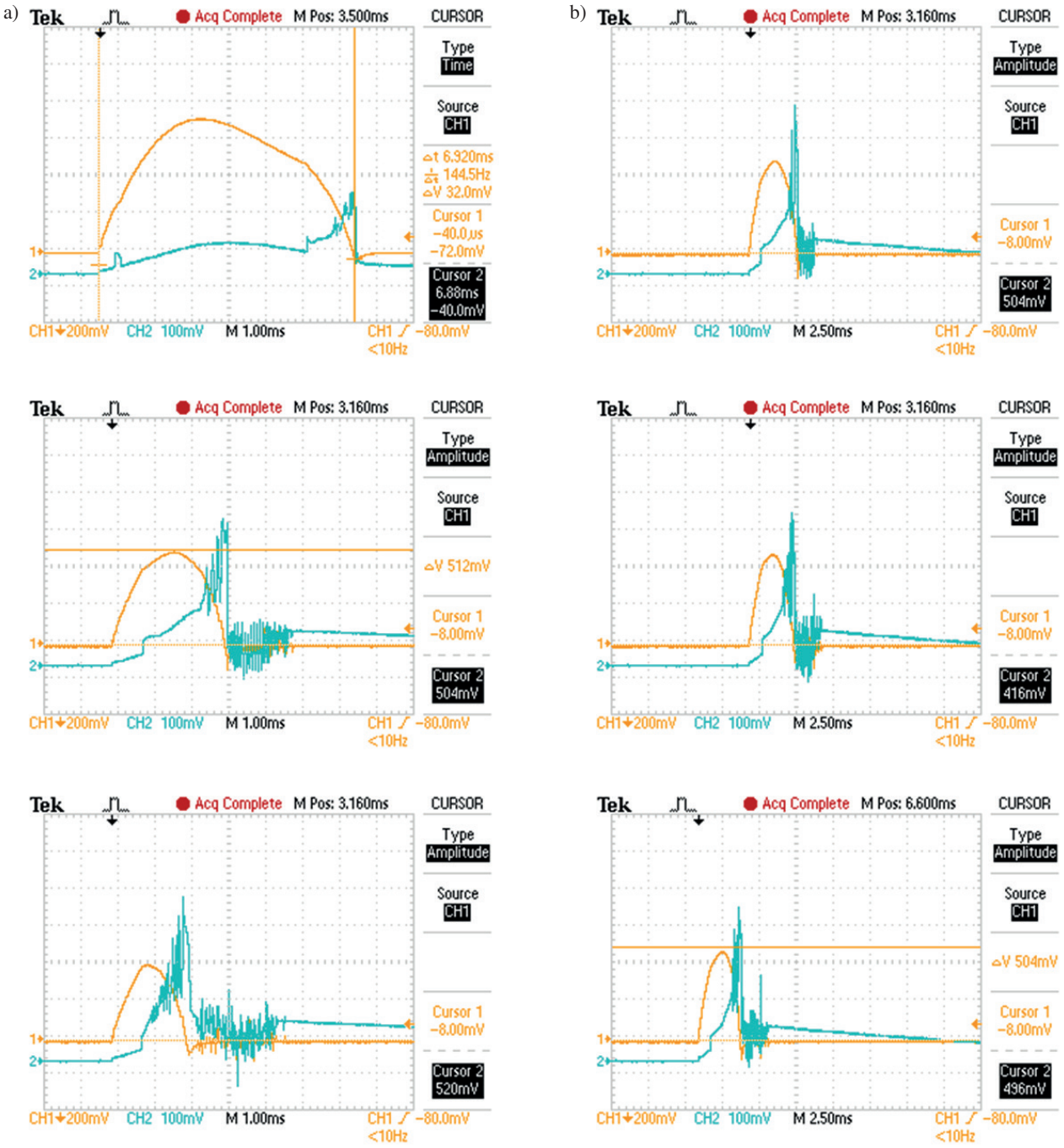

Fig. 11. Exemplary result characteristics of current and voltage during switching off of short-circuit current (screens from the oscilloscope): a) MCB with an arc chamber with 9 plates (negative result); b) MCB with an arc chamber with 13 plates (positive result). The measuring shunt is of our own construction. The shunt is manganese concentric and of resistance equal to 157 μΩ]

erence current characteristic is shown in Fig. 11a); rated voltage equal to 230 V and power factor ($\cos\varphi$) equal to 0.65–0.70. Circuit breakers with arc chamber containing 13 plates disabled the short-circuit current in accordance with the standard in all iterations. 5 iterations were conducted (one iteration for one MCB, total of 25 short-circuit tests). All iterations rendered positive results. Therefore the MCB type with an arc chamber containing 13 plates passed the short-circuit test. Circuit breakers with the arc chamber containing 9 plates did not disable the short-circuit current in accordance with the standard in all iterations. None of the tested devices withstood a full iteration (5 short-circuit tests per MCB). The devices were damaged on the second or third short-circuit test (outcome did not comply with the standard). Therefore the MCB type with the arc chamber containing 9 plates did not pass the short-circuit test. Exemplary results concerning the iterations chosen have been tabularized (Table 1). Exemplary result characteristics saved during the tests are presented in Fig. 11.

Table 1. Exemplary short-circuit tests results for single iterations (pairs of devices from each type). Results for circuit breakers containing 13 and 9 plates in the arc chamber.

Table 1
Short-circuit test results

No.	MCB arc chamber with 13 plates		MCB arc chamber with 9 plates	
	Off time duration [ms]	Value of the short-circuit current [kA]	Off time duration [ms]	Value of the short-circuit current [kA]
1	1.5	1.950	2.0	2.090
2	1.5	3.490	4.5	1.990
3	2.1	2.460	11	2.710*
4	1.5	2.640	–	–
5	1.5	1.900	–	–

* damaged circuit breaker contacts

4.2. Overcurrent protection test. In order to conduct the tests, the TW-1a type transformer was used with a rated voltage of 220 V, frequency equal to 50 Hz and rated power equal to 1 kVA. According to the standard in force (IEC 60898-1), the circuit breakers were tested with the set value of the current equal to 2.8 in for 60 seconds. Five devices from each type were tested. A total of 10 tests was performed. The circuit breakers that contained the arc chamber with 9 plates did not pass the test in any iteration. The circuit breakers that contained the arc chamber with 13 plates passed the test in all iterations.

4.3. Dielectric strength tests. In order to perform the dielectric strength tests, the AP-5 device was used, with the rated test voltage of 5 kV. Circuit breakers were tested using the voltage value of 900 V within 5 seconds. Tests did not indicate the insulation breakdown of the tested MCB containing the arc chamber with 13 plates. In addition, there was no breakthrough of the air gap between the main contacts of the circuit breakers. Therefore the device passed the test. Tests also indicated the insulation breakdown of the tested MCB containing the arc chamber with 9 plates. Breakthrough of the air gap between the main contacts was indicated. Therefore the device did not pass the test.

5. Switching-off cycle procedure and results validation

Switching-off cycle procedure and results were carried out in accordance with standard IEC 60898-1, subsections 9.7.6.3; 9.12.7.1; 9.12.7.3; 9.12.11.2; 9.12.11.3; 9.12.11.4; 9.12.12.1 and 9.12.12.2.

5.1. Test of rated short-circuit breaking capacity (I_{cn}). The tested circuit is scaled accordingly. The test is performed on three samples in the appropriate circuit. If the supply and receiving terminals of the circuit breaker are not properly marked under the test conditions, two samples are connected in one direction and the third in the opposite direction. The switching cycle is being executed: O–t–CO (switch-off; time; switch- on). If 'O' is switched off and the auxiliary switch 'A' synchronizes with the voltage waveforms in such a manner that the circuit closes before switching off the first sample at the moment corresponding to the 15° phase angle. It is made in accordance with standard 67 – EN 60898-1: 2003 + A1: 2004 + A11: 2005. In the case of switching off the second sample, the moment of switching on the circuit is shifted by a phase angle of 30°, and in the case of switching off the third sample – by a further 30° of a phase angle. Sync tolerance should be ±5°. For multi-pole circuit breakers, synchronization should be performed in relation to the same reference pole.

In the case of switching off single-pole switches with rated voltage 230/400 V, the test is performed in the circuit on an additional set of four samples. Three of these samples are included in the test circuit, one in each phase; closing synchronization of the short circuit with auxiliary switch 'A' is not performed. It is forbidden to connect the neutral point of the power supply system to the common point on the load side of the breakers.

5.2. Circuit breaker check after short-circuit testing. Reduced short-circuit currents, at 1 500 A and with operational short-circuit capacity. After each test the switches should not exhibit any damages affecting their further operation and should pass with a positive result, and without maintenance, the tests listed below:

a) Checking the leakage current between open contacts;
b) Checking the dielectric strength, performed from 2 h to 24 h after short-circuit tests, but with the testing voltage reduced by 500 V without prior influence of humidity.

During these tests, it should be checked whether after performing the test under the conditions concerning the specified item the indicators are in the state of opening, and after the test under these conditions their closing status should be verified.

c) In addition, the circuit breakers should not trip when all of the poles are in the cold state under influence of a current equal to 0.85 of the conventional failure current.

At the end of this check, the current should be gradually increased so that it reaches 1.1 times the value of the conventional tripping current within 5 s. The switch should trip within conventional time.

5.3. Circuit breaker check after short-circuit testing. Short-circuit tests at rated short-circuit capacity. After the tests, the polyethylene film should not have holes visible with normal or corrected vision without additional enlargement, and the switches should not show any damages affecting their further operation. Likewise, they should, without maintenance and prior influence of humidity, have positive results of the following tests:

a) Checking the leakage current between open contacts;
b) Checking the dielectric strength, performed from 2 h to 24 h after short-circuit tests, but with 900 V voltage value and without prior humidity influence.

During these tests, it should be checked whether after performing the test under the conditions concerning the specified item the indicators are in the state of opening, and after the test under these conditions their closing status should also be verified.

c) In addition, these switches should trip under a load of a current equal to 2.8 in on all poles during the time corresponding to the test. The lower operating time limit is 0.1 s instead of 1 s but not exceeding 60 s.

MCB detailed dimensions were shown in Fig. 12a.

6. Juxtaposition of theoretical and empirical results

The most important and interesting data concerning empirical work were derived from the short-circuit tests. Negative results manifested themselves in evaporation of contacts, evaporation of the rear sheaths and evaporation of the arc chamber elements. Moreover, those were caused by errors in MCB construction such as: poorly designed arc chamber, incorrect shape of tread electrodes, contact defects and defects of electromagnetic release. The faults listed above are the direct cause for the occurrence of a large amount of very hot gases and soot. They are the reasons for the huge increase in temperature inside the device. The moment the deionizing properties are constrained, reignition of the electric arc occurs, caused directly by returning voltage. Finally, physical damage to the electromagnetic release or to the thermo-bimetallic release occurs. That can be observed in Fig. 12b.

Hence an unsuccessful attempt to switch off the short-circuit current was observed repeatedly for the MCB with the arc chamber containing 9 plates (no overcurrent function).

An important question emerges: how were the theoretical results derived from the FEM simulations reflected in the empirical results? In this case, the contact system was not the object of calculations. Nevertheless, calculations of the distribution of electric potential could prove helpful in the selection and placement of the right solution concerning the engineering of the arc chamber. Simulations showed places which exhibited heterogeneity of the electric field, and thus electric arc exposure (Fig. 5). In Fig. 7, the value of the potential is exceeded for the MCB with the arc chamber that contains 9 plates. Potential in the gap between the consecutive plates always exceeds 20 volts. Judging from the analytical calculations (Eq. (1)) and the engineering empirical data – 18 Volts and 0.5 Ampere are the limiting values for the possibility/restriction of electric arc occurrence. The FEM model reacts correctly to the nominal voltage. The simulations indicated the areas of the device where the arc was not properly extinguished and that is fully reflected in the empirical results (Fig. 12b). The electrical calculations derived in this manner may prove extremely helpful in the optimization process of the construction of modular apparatuses for all ranges of voltage (e.g. vacuum arc chambers solutions).

It would seem that the voltage calculations are most valuable for low voltage modular devices optimization. However, they are not. Heating simulations clearly indicated that the arc chamber is experiencing faults.

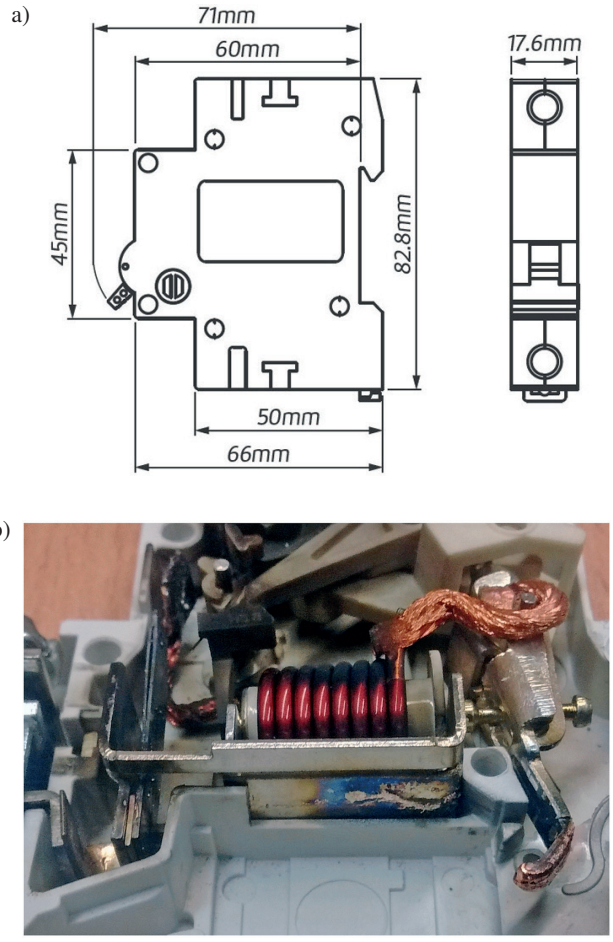

Fig. 12. Empirical results and dimensions of an MCB: a) detailed dimensions of an MCB; b) photo of an MCB with the arc chamber that contained 9 plates. The electric arc has welded the arc chamber to the tread electrodes. The gases generated as a result of electric arc reignition were accumulated in the upper part of the apparatus and then destroyed the thermo-bimetallic plate

The most characteristic is the temperature rise on rear sheaths (Fig. 4b). Moreover, the peak temperature on the plates dividing the arc chamber is indicating electric arc ignition in front of it – this is abnormal. The arc chamber with 13 plates has regular heat distribution. Simulations of this type provide the opportunity to optimize not only the arc chamber but also the other elements of low voltage electrical apparatuses. The possibilities are immense.

An interesting approach was the usage of computational fluid dynamics in terms of electrical apparatuses analysis. Based on the simulations, the functioning and physical phenomena occurring inside the electrical device can be analyzed thoroughly. The CFD module provided not only knowledge about velocity and the distribution of electrically charged particles, but was also useful for the determination of the arc channel placement and therefore the electric arc occurrence.

It is very important to note that the multiple FEM tools used indicated the possibility of electric arc occurrence in the specific areas of the studied circuit breakers. Those areas were common. They also matched those indicated during experimen-

tal studies. Therefore it can be stated that the modeled simulations are emulating and reflecting faithfully the reality and the actual empirical tests that were conducted.

7. Summary

This paper revolves around the construction of an FEM model that could fully and faithfully recreate conditions from reality. The mentioned approach is inestimable when it comes to modelling electrical apparatuses. The approach of using several FEM tools for designing the arc chambers was chosen rightly. However, the optimum possibilities of these tools have been exploited for which they are dedicated in order to receive a valuable and full image of the modelled object. Indeed, this was achieved. The presented model as well as the procedure was verified by empirical studies that confirm the validity of such proceedings. An important feature coming from this work is the possibility of reconstructing the arc chamber models and, in the case of structural changes, avoiding costly and time-consuming laboratory tests or at least reducing the expenses. This approach follows the currently prevailing trend of time and cost reduction in the design and manufacture of electrical equipment. Optimization can be applied to existing solutions using the proposed procedure. Such a process might not only increase the users' safety/service, but also reduce the use of materials, positively affecting the environment. Besides, FEM modeling can be used for designing apparatuses for different conditions, voltage ranges and applications. The above-stated creates vast possibilities for safe, fast and highly economical creation of new trends and solutions in electrical apparatuses engineering. Obviously, the disadvantage of FEM modeling is still an urge to perform experimental tests, as per all the standards in force. Moreover, it should be stressed that in the case of the arc chambers, the modeling is simple and the layout is not complicated. More complex solutions may generate additional errors that can easily lead to major mistakes in designing. This is expected in particular in a boundary conditions setting. Still the proposed modelling procedure is worth employing.

References

[1] R. Bini, B. Galletti, A. Iordanidis, and M. Schwinne, 1st International Conference on Electric Power Equipment – Switching Technology, Xi'an, 2011, pp. 375–378.

[2] L. Wang, H. Liu, W. Zheng, R. Guan, Ch. Ge, L. Chen, and Sh. Jia, "Numerical Simulation of Impact Effect of Internal Gas Pressure on Chamber Housing in Low-Voltage Circuit Breaker", *IEEE Transactions on Components, Packaging and Manufacturing Technology* 4(4), (2014).

[3] X. Ye, M.T. Dhotre, J.D. Mantilla, and S. Kotilainen, "CFD Analysis of the Thermal Interruption Process of Gases with Low Environmental Impact in High Voltage Circuit Breakers", 2015 Electrical Insulation Conference (EIC), Seattle, 2015.

[4] M.T. Dhotre, X. Ye, M. Seeger, M. Schwinne, and S. Kotilainen, "CFD Simulation and Prediction of Breakdown Voltage in High Voltage Circuit Breakers", 2017 Electrical Insulation Conference (EIC), Baltimore, 2017.

[5] B. Qi, X. Zhao, Sh. Zhang, M. Huang, and Ch. Li, "Measurement of the electric field strength in transformer oil under impulse voltage", *IEEE Transactions on Dielectrics and Electrical Insulation* 24, 1256–1262 (2017).

[6] C. Rumpler, H. Stammberger, and A. Zacharias, "Low-voltage arc simulation with out-gassing polymers", *Proc. IEEE 57th Holm Conf. Electr. Contacts*, 2011, pp. 1–8.

[7] V.V. Ryzhov, O.N. Molokanov, P.A. Dergachev, N.A. Vedechenkov, E.P. Kurbatova, and P.A. Kurbatov, "Simulation of the Low – Voltage DC Arc", Intenational Youth Conference on Radio Electronics, Electrical and Power Engineering (REEPE), 2019, Russia.

[8] N.D. Geetha, P. Rasilo, and A. Arkkio, "Sensitivity Analysis of Inverse Thermal Modeling to Determine Power Losses in Electrical Machines", *IEEE Transactions on Magnetics* 54(11), (2018).

[9] J. Li, Y. Cao, M. Y., Sh. Liu, Z. Du, and Y. Feng, "Research on the Effect of Magnetic Field on Micro-Characteristics of Vacumm Arc During Arc Formation Process", 28th International Symposium on Discharges and Electrical Insulation in Vacuum (ISDEIV), 2018, Germany.

[10] P. Tarnowski and W. Ostapski, "Pulse powered turbine engine concept – numerical analysis of influence of different valve timing concepts on thermodynamic performance", *Bull. Pol. Ac.: Tech.* 66 (3), 373–382 (2018).

[11] V.S. Nagarajan, V. Kamaraj, and S. Sivaramakrishnan, "Geometrical sensitivity analysis based on design optimization and multiphysics analysis of PM assisted synchronous reluctance motor", *Bull. Pol. Ac.: Tech.* 67 (1), 155–163 (2019).

[12] R. Bini, N.T. Basse, and M. Seeger, "Arc-induced Turbulent Mixing in a Circuit Breaker Model", *J. Phys D Appl Phys* 44 (2), (2011).

[13] R. Holm, *Electric Contacts – Theory and Application*, NewYork, NY, USA: Springer.

[14] N.P.T. Basse, R. Bini, and M. Seeger, "Measured turbulent mixing in a small-scale circuit breaker model", *Appl. Optics* 48 (32), 6381–6391 (2009).

[15] F.P. Incropera, D.P. DeWitt, T.L. Bergman, and A.S. Lavine, *Introduction to Heat Transfer*, 5th ed. Hoboken, NJ, 2006, USA: Wiley.

[16] P.T. Muller, ' 'Macroscopic electro thermal simulation of contact resistances, Bachelor thesis", RWTH, 2016, Aachen, Germany.

[17] W. Biao, L. Yanyan, and Z. Xiaojun, "Study on detection technology of the contact pressure on the electrical contacts of relays", 26th International Conference on Electrical Contacts (ICEC), 2012, pp. 161 – 164.

[18] X. Sun, B. Su, L. Chen, Z. Yang, and K. Li, "Design and analysis of interior composite-rotor bearingless permanent magnet synchronous motors with two layer permanent magnets", *Bull. Pol. Ac.: Tech.* 65 (6), 833-843 (2017).

[19] M. Kriegelet, X. Zhu, H. Digard, S. Feitoza, M. Glinkowki, et al., "Simulations and Calculations as verification tools for design and performance of high voltage equipment", CIGRE, Paris, France, , A3-210 (2008).

[20] P. Kumar and A. Kale, "3-Dimensional CFD simulation of an internal arc in various compartments of LV/MV Switchgear", Ansys Convergence Conference, 2016.

[21] D.J. Hartland, "Electric contact systems – passing power to the trains", IET Professional Development Course on Electric Traction Systems, 2010, pp. 25–37.

[22] G. Chen, L. Lan, Z. Pan X. Wen, Y. Wang, and Y. Wu, "Electrical erosion test and condition assessment of SF6 CB contact sets", *IET Generation, Transmission & Distribution* 11 (8), 1901–1909 (2017).

[23] J.D. Mantilla, N. Gariboldi, S. Grob, and M. Claessens, "Investigation of the insulation performance of a new gas mixture with extremely low GWP", Electrical Insulation Conference, Philadelphia, 2014.

[24] A.A. Iordanidis and C.M. Franck, "Self-consistent radiation based simulation of electric arcs: Application to gas circuit breakers", *Journal of Physics D: Applied Physics* 41, 135206, (2008).

[25] X. Ye and M.T. Dhotre, "CFD Simulation of Transonic Flow in High Voltage Circuit Breaker", *International Journal of Chemical Engineering*, 2012, Article ID 609486.

[26] H. Kim, I. Chong, and S. Lee, "Analysis of SLF Interruption Performance of Self-Blast Circuit Breaker by Means of CFD Calculation", *Journal of Electrical Engineering & Technology* 9 (1), 254–258 (2014).

[27] M. Lindmayer and H. Stammberger, "Application of numerical field simulations for low-voltage circuit breakers", *IEEE Transactions on Components, Packaging, and Manufacturing Technology: Part A* 18 (3), (1995).

[28] P.U. Frei and H.O. Weichert, "Advanced Thermal Simulation of a Circuit Breaker", *Proceedings of the 50th IEEE Holm Conference on Electrical Contacts and the 22nd International Conference on Electrical Contacts Electrical Contacts* (2004).

[29] S. Ito, Y. Takato, Y. Kawase, and T. Ota, "Numerical analysis of electromagnetic forces in low voltage AC circuit breakers using 3-D finite element method taking into account eddy currents", *IEEE Transactions on Magnetics* 34 (5), (1998).

[30] Ch. Degui, L. Xingwen, J. Liang, and Z. Xin, "Numerical Simulation of Arc Motion During Interruption Process of Low-Voltage Circuit Breakers", ICEC 2012.

[31] P. Kačor and P. Bernat, "Analysis of force characteristic of short-circuit release in low voltage circuit breaker", *Proceedings of the 2014 15th International Scientific Conference on Electric Power Engineering*, (2014).

[32] M. Conecici-Lucian, C. Munteanu, and I.M. Purcar, "3D finite element analysis of a miniature circuit breaker", 6th International Conference on Modern Power Systems MPS2015, Cluj-Napoca, 2015.

[33] L. Chunlei, W. Dong, Z. Bing, L. Jin, and Z. Wenjun, "On Novel Methods for Characterizing the Arc/Contact Movement and Its Relation With the Current/Voltage in Low-Voltage Circuit Breaker", *IEEE Transactions on Plasma Science* 45 (5), 882–888 (2017).

[34] N. Vasiraja and P. Nagaraj, "The effect of material gradient on the static and dynamic response of layered functionally graded material plate using finite element method", *Bull. Pol. Ac.: Tech.* 67 (4), 828–838 (2019).

[35] 1. D. Pop, L. Neamt, R. Tirnovan, and D. Sabou, ' "3D Finite Element Analysis of a Miniature Circuit Breaker", HE 8th International Symposium on Advanced Topics in Electrical Enginnering, Bucharest, 2013.

[36] Ch. Degui, D. Ruicheng, Z. Jingshu, and T. Weixiong, "Dynamic Simulation of Operating Mechanism for Molded Case Circuit Breaker", *Electrical Contacts*, 2007.